Earth Surface Dynamics

Supporting Information for

LONG-TERM PEAT THICKNESS FROM COSMOGENIC Al-26 AND BE-10, HAUTES FAGNES, BELGIAN ARDENNES

Angus Moore[1], Maud Henrion[1], Yanfei Li[1,2], Eléonore du bois d'Aische[1,2], Philip Gautschi[3], Marcus Christl[3], François Jonard[2], Sébastien Lambot[1], Kristof Van Oost[1], Sophie Opfergelt[1], Veerle Vanacker[1,4]

[1]Earth and Life Institute, Université catholique de Louvain, 1348 Louvain-la-Neuve, Belgium

[2]Earth Observation and Ecosystem Modelling Laboratory, Université de Liège, 4000 Liège, Belgium

[3]Laboratory of Ion Beam Physics, ETH Zürich, Zürich, Switzerland

[4]Soil Geography & Landscape Group, Wageningen University, Droevendaalsesteeg 3, P.O. Box 47, 6700 AA, Wageningen, the Netherlands

Contents of this file

Data Availability: All research data, including measured isotopic ratios, Al concentrations, cosmogenic nuclide laboratory data, regolith and solute geochemistry, and stream discharges, as well as the codes used for the inverse-modeling and to make figures are archived in the Zenodo repository (https://doi.org/10.5281/zenodo.18018526).

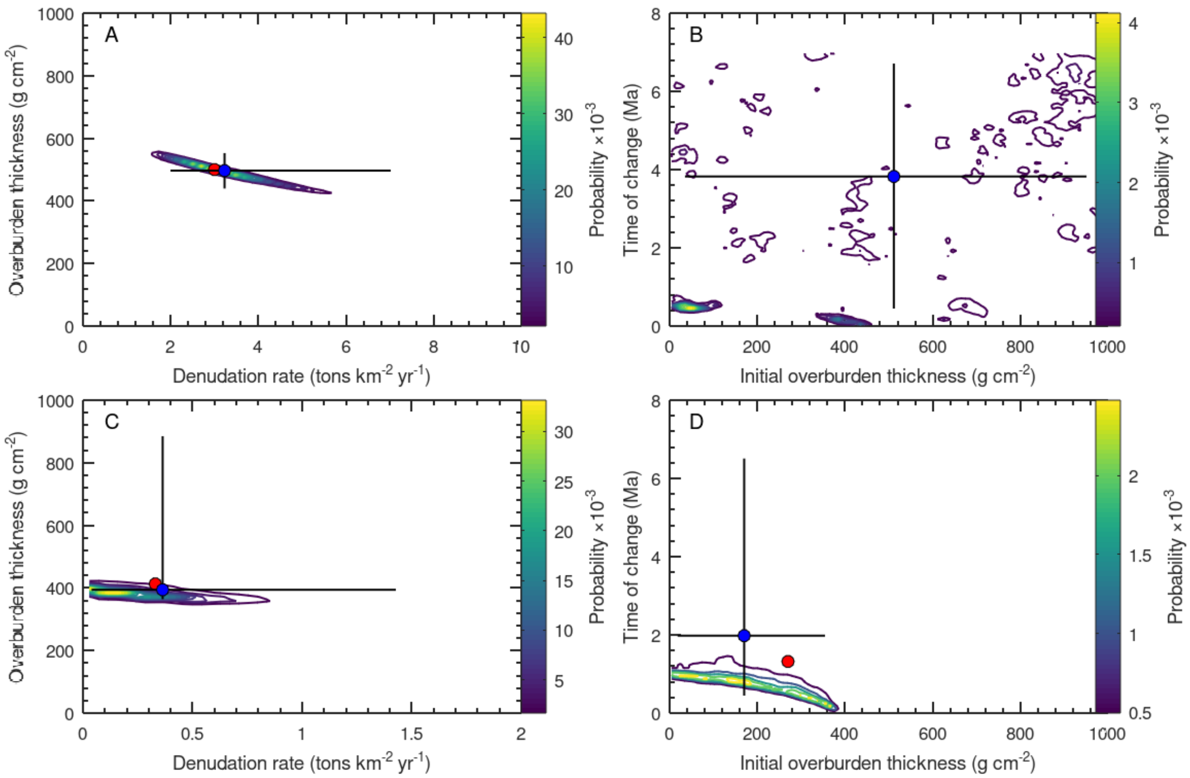

Figure S.1: Joint-distribution plots for two test-cases of the Markov Chain Monte Carlo (MCMC) inversion (main text, section 3.5.4). Red circles show the target parameter values. Blue circles and error bars show the median parameter estimate and 90% confidence interval from the MCMC inversion. Panels A and B show inversion results for a denudation rate of 3 tons km^{-2} yr^{-1} and an overburden thickness of 500 g cm^{-2}, with no change in overburden thickness with time, modeled using Eq. 5. The inversion successfully recovers the target denudation rate and overburden thickness (Panel A), while the timing of the change in overburden thickness and the initial thickness remain unconstrained (Panel B). Panels C and D show the inversion for median parameter values similar to those obtained for LS1 as targets (main text, Table 2). The model returns the parameter values within the 90% confidence interval, although with a greater offset between the median solution and the target values than achieved in the simpler case of no change in overburden thickness (Panel A).

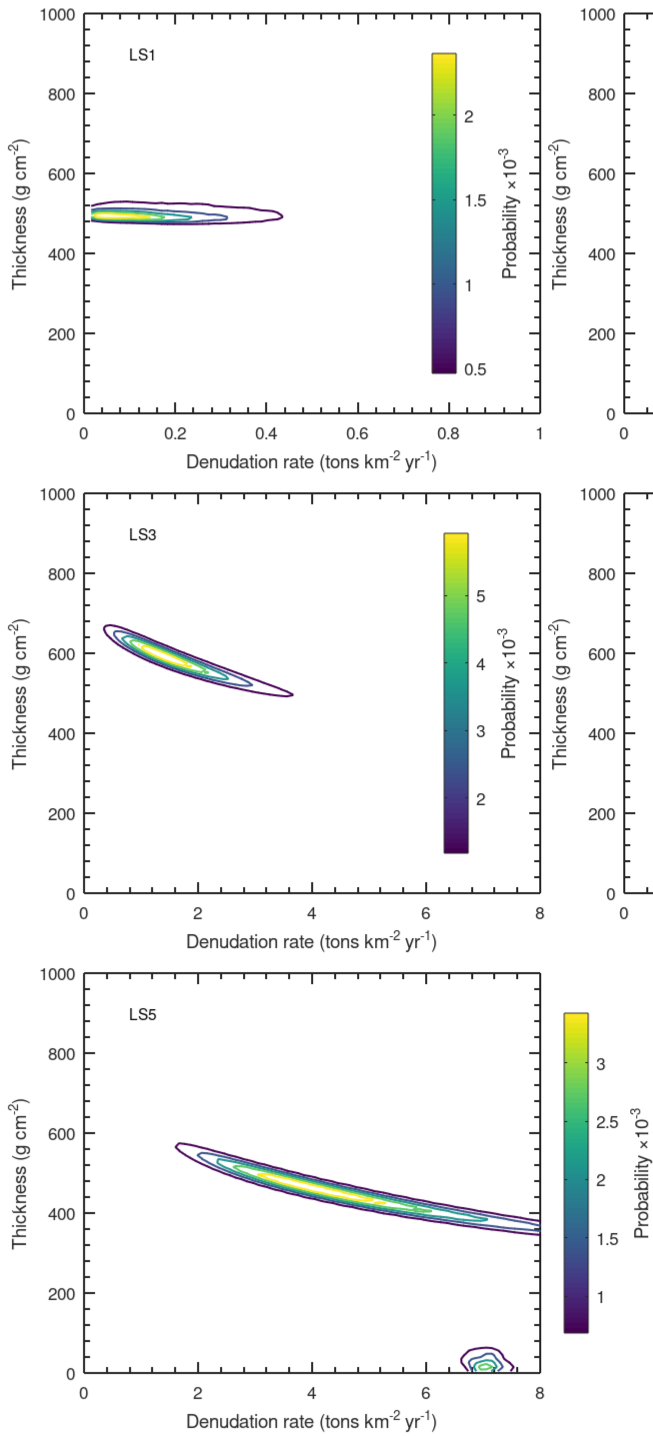

Figure S.2: Joint-distribution plots of overburden thickness vs. denudation rate for the five hillslope positions (LS1-LS5). The overburden thickness and denudation rate covary negatively.

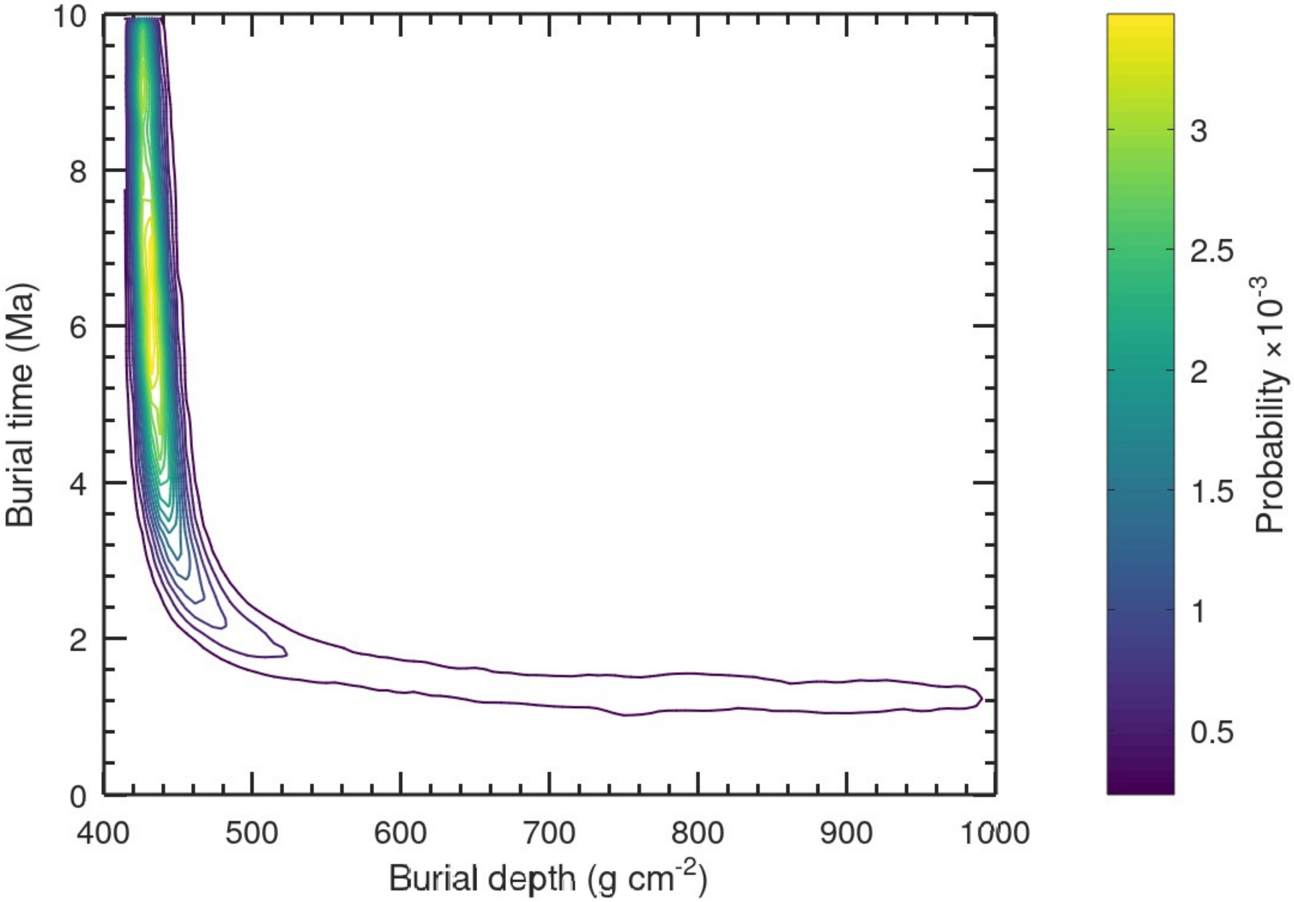

Figure S.3: Joint-distribution plot of the burial time and burial depth inferred from the floodplain sediment model (main text, Eq. 7). The burial time is unconstrained above ca. 1 Myr.

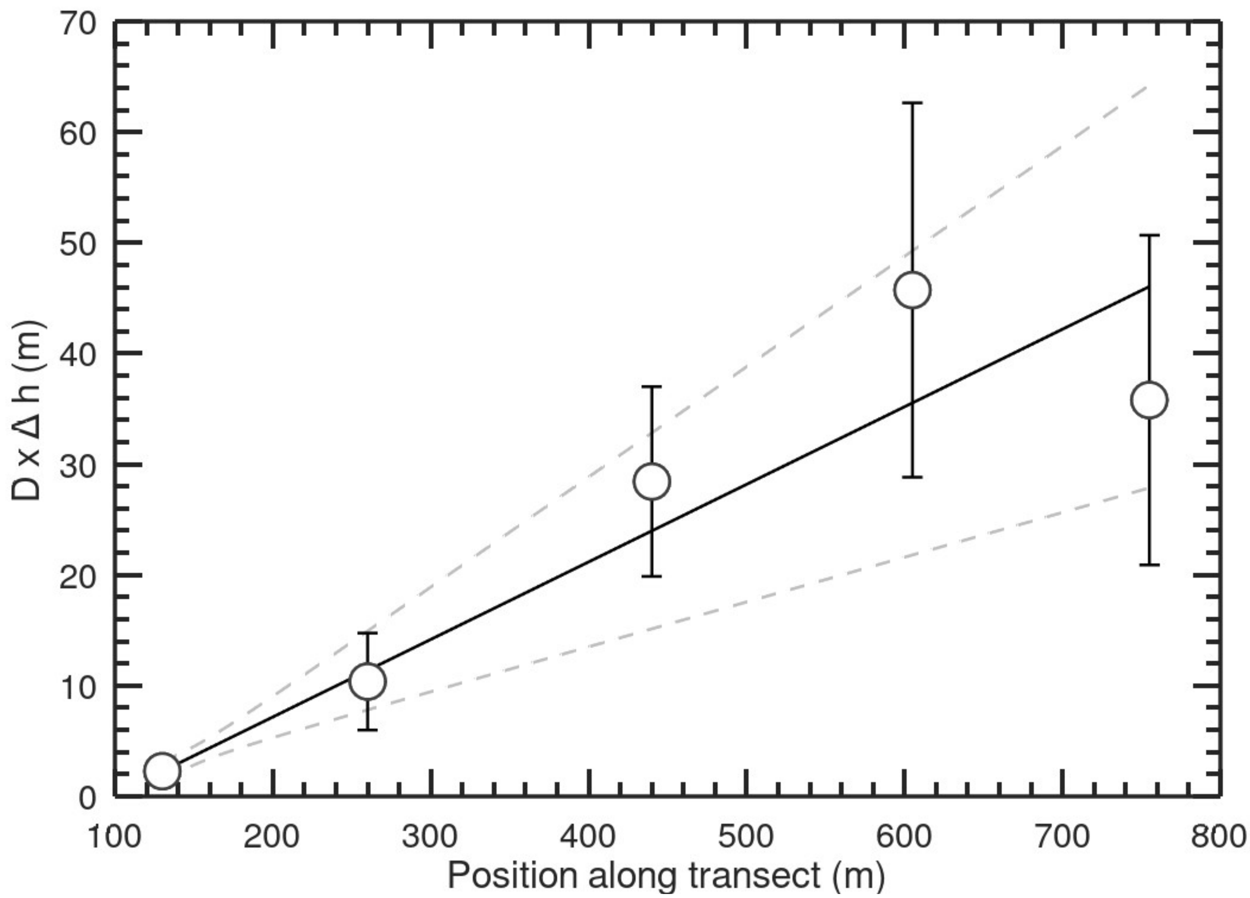

Figure S.4: Plot of the product of modeled peat depth (*D*) and surface/hydraulic head gradient (*Δh*) at LS1-LS5 vs. the downslope position along the transect. If the flow of water through the peat layer is dominated by horizontal flow because of the low permeability of the underlying clay-rich saprolite, and hydraulic conductivity within the peat layer is spatially uniform, then *D x Δh* should increase linearly along the downslope transect to accommodate a linear increase in discharge with distance from the drainage divide (main text, section 6.2). This behavior is observed, supporting that the model results are reasonable for a steady-state peatland.

Supporting Text S.1:

To calculate watershed-averaged denudation rates, we assume that the sampled stream sediment is derived from erosion of quartz-bearing saprolite on the hillslopes and that this material is then transported downslope through the peat layer, which functions as physically mobile regolith. We further assume that the peat layer is vertically mixed over the timescales of downslope transport. We then adopt the approach of Riebe and Granger (2013) with modification to incorporate the effects of radioactive decay. The change in the concentration of a cosmogenic nuclide, N, in quartz from the peat layer with time can be described by the differential equation:

$$\frac{d\langle N\rangle}{dt} = \langle P\rangle [Qtz_{soil}] - \langle N\rangle \frac{E_{soil}}{z}[Qtz_{soil}] - \langle N\rangle \lambda [Qtz_{soil}] + N_{\mathrm{sub}} \frac{E_{sap}}{z}[Qtz_{\mathrm{sub}}] \qquad \text{Eq. S.1}$$

where $<P>$ represents the depth-averaged ^{10}Be or ^{26}Al production rate in quartz in the peat layer (atoms g^{-1} yr^{-1}), $[Qtz_{peat}]$ and $[Qtz_{sap}]$ the concentrations of quartz in the peat layer and the saprolite, $<N>$ the depth-averaged concentration of ^{10}Be or ^{26}Al in quartz in the peat layer (atoms g^{-1}), z the saturated peat layer mass-thickness (g cm^{-2}), λ the decay constant of ^{10}Be or ^{26}Al (yr^{-1}), N_{sap} the concentration of ^{10}Be or ^{26}Al in quartz at the top of the saprolite (atoms g^{-1}), and E_{sap} the erosion flux of saprolite (g cm^{-2} yr^{-1}). The first term on the right-hand side represents *in situ* production in the peat layer, the second term nuclide loss through erosion of the peat layer, the third nuclide loss through radioactive decay, and the fourth nuclide gain through erosion of saprolite.

For a mixed layer, the average production rate in the layer for production reactions that can be approximated as attenuating exponentially with depth is given by:

$$\langle P\rangle = \sum_i \frac{P_{0,i}\Lambda_i}{z}\left(1 - e^{\frac{-z}{\Lambda_i}}\right) \qquad \text{Eq. S.2}$$

where $P_{0,i}$ is the production rate at the surface by reaction i (atoms g^{-1} yr^{-1}) and Λ_i is the mean free path of the radiation responsible for that reaction (g cm^{-2}). If chemical weathering in the saprolite occurs below the penetration depth of most cosmic radiation, the concentration of ^{10}Be or ^{26}Al at the top of the saprolite (N_{sap}) is set by E_{sap} and by the mass-thickness of the peat layer (z):

$$N_{sap} = \sum_i \frac{P_i(0)}{\lambda + E_{sap}/\Lambda_i} e^{\frac{-z}{\Lambda_i}} \qquad \text{Eq. S.3}$$

The erosion rate of the saprolite can be related to the erosion flux from the peat layer using the conservation of mass of quartz, wherein the mass of quartz entering the peat layer from below must equal the mass leaving by physical erosion:

$$E_{\mathrm{sub}} = E_{soil}\frac{[Qtz_{soil}]}{[Qtz_{\mathrm{sub}}]} \quad \text{Eq. S.4}$$

Assuming steady state, substituting Eqs. S.2 through S.4 into S.1, and rearranging gives an expression for the ^{10}Be or ^{26}Al concentration in quartz as a function of E_{sap}, the peat layer thickness, and the enrichment of quartz across the saprolite-peat layer interface (R) (here Eq. S.5, main text Eq. 6):

$$\langle N \rangle = \sum_i \frac{P_i(0)\Lambda_i}{z}\left(1 - e^{\frac{-z}{\Lambda_i}}\right)\left[\frac{E_{sap}}{\rho h R} + \lambda\right]^{-1} + \frac{E_{sap}}{Rz}\frac{P_i(0)}{\left(\lambda + \frac{E_{sap}}{\Lambda_i}\right)} e^{\frac{-z}{\Lambda_i}}\left[\frac{E_{sap}}{zR} + \lambda\right]^{-1} \quad \text{Eq. S.5}$$

Supporting Text S.2:

The signal averaging timescales presented in Table 2 were calculated using the denudation rates for the hillslope transect positions determined from the Markov Chain Monte Carlo inversion as follows:

$$t_{avg} = \frac{1}{C_{Total}} \sum_i \frac{C_i}{\lambda_n + \frac{D}{\Lambda_i}} \quad \text{Eq. S.6}$$

where t_{avg} is the integration timescale of the signal, C_{Total} is the total cosmogenic nuclide concentration under the steady-state denudation rate, and C_i is the concentration attributable to production mechanism i. The summation is over all production functions.